

Phase Separation, Charge-Density Waves, and Magnetism in $\text{La}_2\text{NiO}_{4+\delta}$ with $\delta = 0.105$

J. M. Tranquada

Brookhaven National Laboratory, Upton, New York 11973

D. J. Buttrey and D. E. Rice

Department of Chemical Engineering, University of Delaware, Newark, Delaware 19716

(Received 21 September 1992)

Neutron diffraction measurements on a highly doped single crystal of $\text{La}_2\text{NiO}_{4+\delta}$ ($\delta = 0.105$) reveal that below room temperature the crystal undergoes phase separation into an orthorhombic structure, with a doubled unit cell along c , and a tetragonal phase. The lattice distortion in the orthorhombic phase suggests charge-density-wave order, and related diffuse scattering is observed at room temperature. The orthorhombic phase orders antiferromagnetically below 55 K with a significant ordered moment ($\sim 0.7\mu_B$).

PACS numbers: 61.12.-q, 71.45.Lr, 75.25.+z

$\text{La}_2\text{NiO}_{4+\delta}$ has received considerable attention over the last few years [1] largely because of its close association with the high-temperature superconducting system $\text{La}_2\text{CuO}_{4+\delta}$ [2]. While the structural phase diagrams of the two systems have strong similarities, the transport properties of these materials are strikingly different. Whereas the cuprate system becomes metallic and superconducting for $\delta \gtrsim 0.03$, the nickelate remains an insulator even for $\delta > 0.1$. The insulating behavior of highly doped lanthanum nickelate poses a significant problem for standard approaches to electronic structure calculation. One recent study [3] suggested that holes added to La_2NiO_4 might be localized by a breathing-mode distortion of the in-plane oxygens. For the related system $\text{La}_{2-x}\text{Ba}_x\text{CuO}_4$, it has been argued [4] that suppression of superconductivity at $x \approx 0.12$ may involve an in-plane charge-density wave (CDW) that couples to tilts of the CuO_6 octahedra.

In the course of a detailed reexamination of the phase diagram of $\text{La}_2\text{NiO}_{4+\delta}$ [5], we have discovered clear evidence of a commensurate charge-density-wave state involving a doubling of the unit cell along the c axis. Superlattice peaks corresponding to antiferrodistortive displacements of the NiO_6 octahedra appear when a single crystal with $\delta = 0.105$ is cooled below a temperature of ~ 270 K. To our knowledge, this is the first case of a structural unit-cell doubling along c in a K_2NiF_4 -type compound; the only example of such a magnetic, but not structural, doubling occurs in Ca_2MnO_4 [6]. At room temperature, the existence of diffuse scattering with a structure factor similar to the low-temperature ordered phase suggests that local CDW distortions survive to significantly higher temperatures. Consistent with the putative CDW displacements, several transport studies of $\text{La}_2\text{NiO}_{4+\delta}$ indicate a gradual transition from insulating to metallic-like behavior on heating near 500 K [7].

As indicated in Fig. 1, the development of long-range CDW order in the $\delta = 0.105$ crystal involves phase sep-

aration. The sample is tetragonal at room temperature, but separates into the orthorhombic, distorted state plus a tetragonal phase at or below 270 K. The orthorhombic phase exhibits antiferromagnetic order with a substantial ordered moment below a Néel temperature of 55 K, while no magnetic or nuclear superlattice peaks related to the higher δ tetragonal phase have been identified.

Sample preparation is discussed in detail elsewhere [5]. Briefly, several crystals, obtained from a boule grown congruently by rf induction skull melting, were annealed together at 1200 °C in 0.50 atm O_2 for 5 h and quenched to achieve the desired stoichiometry. One of the crystals ($V \approx 0.3 \text{ cm}^3$) was selected for the neutron scattering study. Triplicate iodometric analyses were performed on other material from this anneal to obtain $\delta = 0.105 \pm 0.003$.

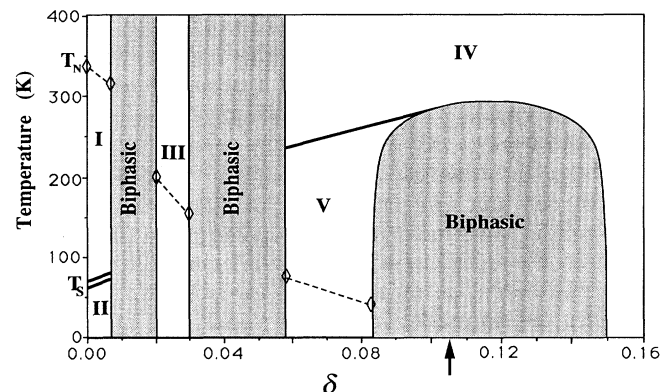


FIG. 1. Phase diagram of $\text{La}_2\text{NiO}_{4+\delta}$ from Ref. [5]. Solid lines indicate structural phase boundaries; diamonds connected by dashed lines indicate Néel temperatures. These results are derived from a combination of synchrotron x-ray powder diffraction and single-crystal neutron diffraction measurements. Similar results for $\delta \lesssim 0.08$ have been obtained by Yamada and co-workers [8]. The arrow indicates the average δ of the sample studied in the present work.

The structure of the crystal was studied by neutron diffraction using the H8 triple-axis spectrometer at the High Flux Beam Reactor at Brookhaven National Laboratory. The (002) reflection of pyrolytic graphite (PG) was used for the monochromator, together with one or two PG filters to eliminate $\lambda/2$ contamination. Most of the results reported here were measured with an incident energy of 14.7 meV. For high Q resolution, horizontal collimations of $20'-10'-10'-20'$ with a PG (004) analyzer were selected, while the collimations were relaxed to $40'-40'-80'-80'$ to gain intensity for measuring the diffuse scattering. The crystal was sealed in an Al can with He exchange gas, and fastened to the cold finger of a Displex closed-cycle He refrigerator. Some results were checked by x-ray diffraction at beam line X7 at the National Synchrotron Light Source, also at Brookhaven, on a powder sample ground from crystalline material annealed under the same conditions as the crystal used in the neutron study.

The c axis is chosen to be the long axis of the unit cell, perpendicular to the NiO_2 planes. In both the tetragonal and orthorhombic phases, the in-plane Ni-O bonds lie along the $[110]$ and $[1\bar{1}0]$ directions. The crystal was oriented with a $[100]$ axis vertical, allowing measurement of all reflections of the form $(0kl)$ [and, because of twinning, $(h0l)$].

The signature of the CDW phase is a set of superlattice peaks at positions $(0kl/2)$ with k and l odd [9]. [Peaks at $(h0l/2)$, with h and l odd, are much weaker. No peaks are observed for l even and k or h odd for either the orthorhombic or tetragonal phase.] High resolution measurements definitively show that the superlattice peaks are associated with the orthorhombic phase. The condition that k (h) and l must be odd indicates that the pattern of atomic displacements must be antiferrodistortive both within the planes and along c . Structure factors obtained from integrated intensities for $(0kl/2)$ reflections measured at 8 K are shown in Fig. 2. The difference in intensity patterns for $k = 1$ and 3, together with the observation that $I(0kl/2) \gg I(h0l/2)$, suggests that the octahedra are tilted along $[010]$.

The highest-symmetry space group that allows 8 Ni atoms per unit cell and tilting of the NiO_6 octahedra is $Pm2_1b$. This low-symmetry space group forces us to include the anticipated symmetries through the choice of coordinates, as indicated in Table I. (Note that we neglect the interstitial oxygens. Different superlattice peaks have been observed by electron diffraction and interpreted in terms of ordering of interstitial oxygen by Hiroi *et al.* [10].) Structural parameters were determined by a least-squares fit to fourteen fundamental and seventeen superlattice reflections [11]. Although the superlattice peaks are weak, the strongest being only $\sim 1\%$ of the stronger fundamental reflections, their intensities are entirely dependent on the distortions of the CDW state. The $(0kl/2)$ intensities can be fitted fairly well by a

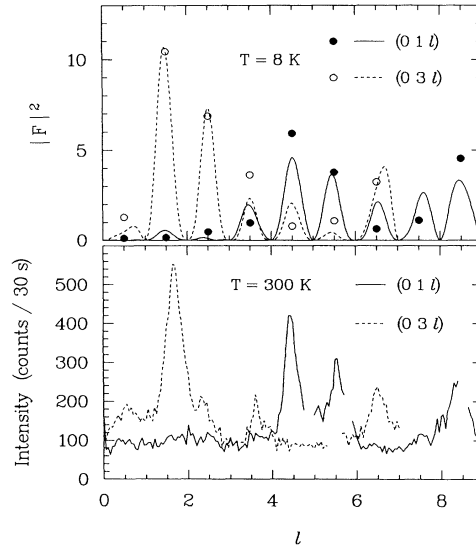


FIG. 2. Upper panel: square of the structure factor obtained from integrated intensities at $T = 8$ K (symbols), and calculated from the structural model (lines). Lower panel: diffuse elastic scattering measured along the $(01l)$ and $(03l)$ rods at 300 K; gaps occur where diffraction peaks due to the Al sample holder have been deleted.

rotation of the octahedra by $\sim 2.5^\circ$ about the $[100]$ axis, with the tilt direction alternating along $[010]$ and $[001]$ directions. However, tilts alone leave the $(h0l/2)$ intensities zero. To obtain finite $(h0l/2)$ peaks, and a small reduction of χ^2 , we include symmetric breathing-mode distortions of the NiO_6 octahedra. The relative signs of the resulting parameters indicate that the apical oxygens move in towards Ni when the in-plane oxygens move out, and vice versa for the nearest-neighbor octahedra.

The parameters in Table I are only approximate—a more complete and accurate description of the distortions will require measurements on a single phase sample. Nevertheless, the salient point here is that the observed superlattice peaks imply a significant reduction in symmetry in the orthorhombic phase. Neighboring NiO_6 octahedra become inequivalent, consistent with a CDW state.

Below ~ 55 K we observe an extra set of superlattice peaks associated with the orthorhombic phase and due to magnetic order. The spin structure has a propagation vector and spin direction parallel to $[100]$, just as in stoichiometric La_2NiO_4 [12–14]. The product of the ordered moment and the magnetic form factor, $\langle M \rangle_0 f(Q)$, extracted from integrated intensities measured at 8 K is shown in Fig. 3; the temperature dependence of the ordered moment is plotted in the inset. Although not definitive, the form factor appears to have a weaker plateau at small Q than that observed in stoichiometric La_2NiO_4 [15]. Allowing for uncertainty in the form factor, we estimate the low-temperature ordered moment

TABLE I. Atomic coordinates for model of orthorhombic CDW phase in $\text{La}_2\text{NiO}_{4.105}$ using space group $Pm2_1b$ (No. 26) with eight formula units per unit cell; lattice parameters at 8 K are $a = 5.435 \text{ \AA}$, $b = 5.497 \text{ \AA}$, and $c = 25.19 \text{ \AA}$. The coordinates of $Pm2_1b$ are obtained from those of $Pmc2_1$ by the permutation $\mathbf{abc} \rightarrow \mathbf{a\bar{c}b}$, which is equivalent to \mathbf{acb} .

Atom	Wyckoff position	Coordinates			Parameter values
		x	y	z	
Ni	2a	0	0	$-\frac{3}{8}$	
	2b	$\frac{1}{2}$	$\frac{1}{2}$	$\frac{1}{8}$	
	2a	0	0	$\frac{1}{8}$	
	2b	$\frac{1}{2}$	$\frac{1}{2}$	$-\frac{3}{8}$	
O(1)	4c	$\frac{1}{4} - \delta y_{O1}$	$\frac{1}{4} - \delta y_{O1}$	$-\frac{3}{8} - z_{O1}$	$\delta y_{O1} = 0.0036$
	4c	$\frac{1}{4} - \delta y_{O1}$	$\frac{1}{4} + \delta y_{O1}$	$\frac{3}{8} - z_{O1}$	$z_{O1} = 0.0022$
	4c	$\frac{1}{4} + \delta y_{O1}$	$\frac{1}{4} + \delta y_{O1}$	$\frac{1}{8} + z_{O1}$	
	4c	$\frac{1}{4} + \delta y_{O1}$	$\frac{1}{4} - \delta y_{O1}$	$-\frac{1}{8} + z_{O1}$	
O(2)	2a	0	y_{O2}	$-\frac{3}{8} + z_{O2} + \delta z_{O2}$	$y_{O2} = 0.0221$
	2a	0	$-y_{O2}$	$-\frac{3}{8} - z_{O2} - \delta z_{O2}$	$z_{O2} = 0.0811$
	2b	$\frac{1}{2}$	$\frac{1}{2} + y_{O2}$	$\frac{1}{8} + z_{O2} + \delta z_{O2}$	$\delta z_{O2} = 0.0034$
	2b	$\frac{1}{2}$	$\frac{1}{2} - y_{O2}$	$\frac{1}{8} - z_{O2} - \delta z_{O2}$	
	2a	0	$-y_{O2}$	$\frac{1}{8} + z_{O2} - \delta z_{O2}$	
	2a	0	y_{O2}	$\frac{1}{8} - z_{O2} + \delta z_{O2}$	
	2b	$\frac{1}{2}$	$\frac{1}{2} - y_{O2}$	$-\frac{3}{8} + z_{O2} - \delta z_{O2}$	
	2b	$\frac{1}{2}$	$\frac{1}{2} + y_{O2}$	$-\frac{3}{8} - z_{O2} + \delta z_{O2}$	
La	2a	0	y_{La}	$-\frac{3}{8} + z_{La} + \delta z_{La}$	$y_{La} = -0.0060$
	2a	0	$-y_{La}$	$-\frac{3}{8} - z_{La} - \delta z_{La}$	$z_{La} = 0.1777$
	2b	$\frac{1}{2}$	$\frac{1}{2} + y_{La}$	$\frac{1}{8} + z_{La} + \delta z_{La}$	$\delta z_{La} = 0.0005$
	2b	$\frac{1}{2}$	$\frac{1}{2} - y_{La}$	$\frac{1}{8} - z_{La} - \delta z_{La}$	
	2a	0	$-y_{La}$	$\frac{1}{8} + z_{La} - \delta z_{La}$	
	2a	0	y_{La}	$\frac{1}{8} - z_{La} + \delta z_{La}$	
	2b	$\frac{1}{2}$	$\frac{1}{2} - y_{La}$	$-\frac{3}{8} + z_{La} - \delta z_{La}$	
	2b	$\frac{1}{2}$	$\frac{1}{2} + y_{La}$	$-\frac{3}{8} - z_{La} + \delta z_{La}$	

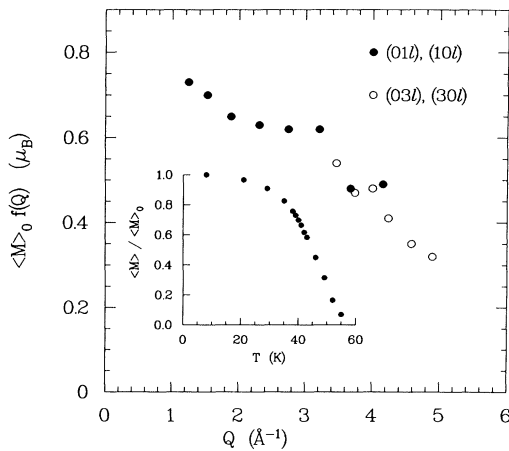


FIG. 3. Magnetic form factor of Ni obtained at $T = 8 \text{ K}$ from antiferromagnetic Bragg peak intensities. Inset shows the temperature dependence of the ordered magnetic moment, obtained from the (011) peak intensity.

to be $(0.75 \pm 0.1)\mu_B$.

While writing this paper, we became aware that the CDW superlattice peaks had been observed previously by Pintschovius *et al.* [16]. However, their crystal had a poorly controlled stoichiometry, since they reported a formula of $\text{La}_{1.9}\text{NiO}_{3.87}$. That crystal was found to be tetragonal, with no magnetic order. The significance of the lattice distortion was missed in that work.

After having identified the orthorhombic CDW phase, we looked for diffuse scattering along the (01 l) and (03 l) rods above the phase separation temperature. The results are shown in the bottom panel of Fig. 2. The diffuse scattering is qualitatively quite similar to the structure factor for a single unit cell of the ordered CDW phase shown in the upper panel. The comparison suggests that lamellar domains of the CDW structure are present within the tetragonal phase, with a correlation length of roughly one unit cell along the c axis. A scan across the rod yields a quasi-Lorentzian line shape with

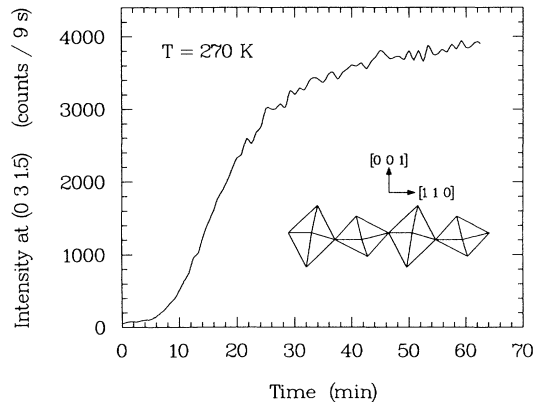


FIG. 4. Time dependence of scattered intensity at $(0\ 3\ 1.5)$ observed with the sample temperature held fixed at 270 K. Inset shows the distortions of the oxygen octahedra along a chain of nearest-neighbor Ni sites; the displacements of the oxygens are exaggerated by a factor of 5.

a width corresponding to a correlation length of ~ 100 Å within the NiO_2 planes.

The x-ray measurements indicate that at low temperature the sample contains $\sim 70\%$ of the orthorhombic phase and 30% of the high- δ phase. We believe that the phase separation results in oxygen-poor and oxygen-rich phases with $\delta \approx 0.08$ and 0.15 [5]. From the proposed phase diagram, the orthorhombic CDW phase appears to cover the composition range $0.06 \leq \delta \leq 0.08$ (see Fig. 1, phase V). Since there are eight Ni sites per unit cell in this phase, it is tempting to associate it with an ideal composition at $\delta = 0.0625$, corresponding to one hole per unit cell.

The phase separation process occurs rather slowly. After cooling from 300 to 270 K, it took roughly 1 h for the intensity of a superlattice peak to saturate, as shown in Fig. 4. Hysteretic behavior was also observed: the superlattice peaks were still present on warming to 290 K. On cooling rapidly from room temperature to 10 K (in a period of ~ 2 h), the CDW peaks were significantly broader than resolution, but annealing at 270 K gave sharp peaks. The phase separation process is probably limited by the rate of diffusion of oxygen; however, there may also be some competition between minimizing the strain energies due to the interstitial oxygens and developing the ordered CDW state. The transition appears to be driven by the electronic energy gains of achieving the CDW order, rather than ordering of the interstitial oxygen.

We gratefully acknowledge helpful discussions with D. E. Cox, V. J. Emery, J. Hriljac, and G. Shirane. Work

at Brookhaven was carried out under Contract No. DE-AC02-76CH00016, Division of Materials Sciences, U.S. Department of Energy. D.J.B. and D.E.R. acknowledge support from the National Science Foundation under Contract No. DMR-891408.

- [1] G. Aeppli and D. J. Buttrey, *Phys. Rev. Lett.* **61**, 203 (1988); J. D. Jorgensen, B. Dabrowski, S. Pei, and D. G. Hinks, *Phys. Rev. B* **40**, 2187 (1989); J. Rodríguez-Carvajal, M. T. Fernández-Díaz, and J. L. Martínez, *J. Phys. Condens. Matter* **3**, 3215 (1991).
- [2] P. M. Grant *et al.*, *Phys. Rev. Lett.* **58**, 2482 (1987); J. D. Jorgensen *et al.*, *Phys. Rev. B* **38**, 11 337 (1988); C. Chailout *et al.*, *Physica (Amsterdam)* **158C**, 183 (1989).
- [3] V. I. Anisimov, M. A. Korotin, J. Zaanen, and O. K. Andersen, *Phys. Rev. Lett.* **68**, 345 (1992).
- [4] S. Barišić and J. Zelenko, *Solid State Commun.* **74**, 367 (1990).
- [5] D. E. Rice and D. J. Buttrey, *J. Solid State Chem.* (to be published); D. J. Buttrey, D. E. Rice, V. Sachan, and J. M. Tranquada (unpublished).
- [6] D. E. Cox, G. Shirane, R. J. Birgeneau, and J. B. MacChesney, *Phys. Rev.* **188**, 930 (1969).
- [7] D. J. Buttrey and J. M. Honig, in *Chemistry of High Temperature Superconductors*, edited by C. N. R. Rao (World Scientific, Singapore, 1991), pp. 283–305, and references therein.
- [8] K. Yamada and Y. Endoh (private communication).
- [9] A check of the $(hk0)$ zone revealed no additional superlattice peaks.
- [10] Z. Hiroi, T. Obata, M. Takano, Y. Bando, Y. Takeda, and O. Yamamoto, *Phys. Rev. B* **41**, 11 665 (1990).
- [11] The fundamental orthorhombic $(h0l)$, $(0kl)$ peaks were resolved, and were separated from the tetragonal contributions by peak fitting; $(00l)$ peaks were not used. Equal weights of the two twin domains were assumed. An extinction correction was included in the fit, but Debye-Waller factors were neglected. The latter choice was motivated by the relatively small Q values for measured reflections, and the desire to limit the number of fitting parameters.
- [12] G. H. Lander, P. J. Brown, J. Spalek, and J. M. Honig, *Phys. Rev. B* **40**, 4463 (1989).
- [13] T. Freltoft, D. J. Buttrey, G. Aeppli, D. Vaknin, and G. Shirane, *Phys. Rev. B* **44**, 5046 (1991).
- [14] The spin direction is determined by the absence of the $[100]$ reflection. It should be noted that the nuclear and magnetic superlattice peaks occur at different values of l , and hence do not overlap.
- [15] X.-L. Wang *et al.*, *Phys. Rev. B* **45**, 5645 (1992).
- [16] L. Pintschovius, J. M. Bassat, P. Odier, F. Gervais, G. Chevrier, W. Reichardt, and F. Gompf, *Phys. Rev. B* **40**, 2229 (1989).